Dynamic polymer hydrogels as synthetic extracellular matrices for 3D cell culture

Liu, T.

CHAPTER 5

Engineering macroporous hydrogels using the tetrazine-norbornene click reaction

This chapter is prepared as an original research paper: Tingxian Liu, Wei Tang, Roxanne E. Kieltyka*

5.1 Abstract

Macropores play critical role in transport and exchange of nutrition, oxygen and waste for cells, influencing parameters such as cell morphology, growth, migration and differentiation. However, approaches to engineer the user-defined macropores in a controlled manner in synthetic hydrogel materials remains to be explored. In this study, the inverse electron demand Diels–Alder (IEDDA) reaction that is known as an efficient chemical reaction for bioconjugation and crosslinking due to its fast kinetics, orthogonality and biocompatibility, is employed to engineer macroporous hydrogel structures from nitrogen gas that is formed in the IEDDA reaction in the hydrogelation process. To tune the pore size, I synthesized tetrazine derivatives with substituents that vary in electron donating character on a poly(ethylene glycol) PEG macromonomer and examined their reaction with a second PEG macromonomer containing norbornene groups (Tz-Nb reaction) to generate hydrogel materials of varied stiffness and stable macropores arising from the simultaneous gas formation in the cross-linking reaction. Hydrogen-substituted tetrazines (TZ3) displayed faster reaction kinetics and hydrogelation over those bearing methyl or methylene substituents on the tetrazine ring as demonstrated by oscillatory rheology. The faster gelation of the Tz3-Nb-based PEG hydrogel minimized coalescence of the bubbles during their formation, resulting in hydrogels with significantly smaller pores with an average diameter of 268 $\pm$ 94 μm in comparison to the slower reacting Tz2-Nb-based PEG hydrogels (382 $\pm$ 99 μm). Moreover, the faster gelation process of Tz3-Nb crosslinks prevented cell sedimentation, providing a three-dimensional distribution of cells throughout the hydrogel. Additionally, the Tz-Nb-based PEG hydrogels supported the culture of primary chondrocytes with high cell viability and secretion of glycosaminoglycans demonstrating their potential for chondrocyte culture. Overall, we disclose a chemical method to control hydrogel macropore size by tuning the rate of Tz-Nb reaction, and

examine their potential for supporting cartilage matrix production during 3D cell culture.

5.2 Introduction

The development of biocompatible synthetic polymer materials has promoted the progress of biomedical fields that involve engineering of the cell microenvironment *in vitro* such as 3D cell culture, drug discovery, cancer therapy and tissue regeneration.[1–4] Synthetic polymer scaffolds or hydrogels that imbibe large quantities of water have been widely studied in this area because of their capacity to mimic the water-rich character of native tissues. To closely engineer the native microenvironment, hydrogels are designed with both biochemical and biophysical cues for in vitro cell culture relying on cell-binding peptides for cell adhesion and proliferation, dynamic or degradable crosslinks to support matrix remodeling, and mechanical stiffness to guide cell morphological changes, migration, and even stem cell differentiation.[5–7] Among all hydrogel parameters, the pore size is an essential one that can dramatically influence cell behaviour through providing sufficient nutrition and oxygen transport, exchange of waste compounds and space for growth of extracellular matrix components. Biomedical applications involving vascularization, wound healing, bone tissue regeneration, stem cell differentiation or maturation have demonstrated the need for pore sizes in the micron range, for example, pores with 100 µm diameter fully support mesenchymal stem cell adhesion while larger pores (325 µm) facilitate cell migration.[8–13]

Beside the pore size that guides cell behaviour via the interface between cells and pores, their distribution within the materials or their porosity, the pore volume over the total hydrogel volume, can also be envisaged to influence cell behaviour. Even by increasing the pore size and pore densities, hydrogel porosity can be increased, their homogeneity and structural information will also be critical to engineering porous

materials for biological applications.[14] In order to better understand the potential to tune these parameters in synthetic materials, several approaches to generate pores with diameters from several to several hundred micrometers have been reported.[15,16] Salt particles (sodium chloride) or porogens (*e.g.* sodium hydrogen carbonate, silica and agarose beads) in the polymer solutions for hydrogelation have been applied in combination with particulate leaching or dissolution to modulate pore size.[17] Freeze drying is another technique that has been examined for pore formation that makes use of ice crystal formation that occurs with rapid cooling. Additionally, gas forming reactions have emerged as an inexpensive and efficient way to intentionally introduce macropores into hydrogels by using blowing agents such as sodium and ammoniun bicarbonate.[18] While macropores can be generated, these approaches are challenged for use in cell culture where 3D encapsulation is involved. In contrast, the unintentional formation of pores has been observed in 3D bioprinting with VA-086, a photoinitiator that generates nitrogen gas on decomposition with light.[19] Although the photointiator is efficient in improving the cell viability during the bioprinting, the formed hydrogels are turbid due to the trapped gas bubbles. Though the amount of gas formed can be tuned by varing the initiator concentration, the simultaneous generation of radicals to crosslink the polymers can limit its applicability. Therefore, a biocompatible strategy that would provide a handle for controlled bubble formation is very attractive to engineer macroscale pores in hydrogels in a user-defined manner.

The Inverse electron demand Diels–Alder (IEDDA) reaction stands out for the construction of hydrogel materials because of its capacity to form covalent bonds with high selectivity and robust kinetics under physiological conditions.[20–22] The IEDDA reaction proceed with significantly improved secondary reaction constants ranging from hundreds to thousands and in comparison to conventional click reactions, does not require the use of metals as catalysts.[23,24] As a bioconjugation strategy, the IEDDA reaction has also been used to introduce of bioactive peptide or protein cues for

binding to cells, fluorescent labels for live cell imaging, and to engineer degradable or dynamic building blocks in biomaterials.[25–27] Moreover, bioorthogonal hydrogels that based on IEDDA-crosslinkable polymers including polyethylene glycol (PEG), alginates, hyaluronic acid and poly(styrene-alt-maleic anhydride) have been shown to be efficient for drug delivery, cell encapsulation and 3D cell culture.[28–32] The IEDDA reaction mechanism consists of the [4+2] cycloaddition of 1,2,4,5-tetrazines and various dienophiles generating dihydropyridazines as an intermediate product that transform into pyridazines with oxidation and the formation of N_2 gas. When combined with hydrogelating polymers macro-sized pores have been observed from IEDDA reactions according to cryo-scanning electron microscopic images, but the use of this reaction to tune the pores within the hydrogels has not been examined thus far.[29] Due to the large number of IEDDA reaction pairs available that possess different reactivity, reaction kinetics and stability, the door is open to control the formation of macropores within these materials for a range of 3D cell culture applications.

We therefore became interested to understand the potential for tuning macropore size and distribution within the hydrogel materials by tuning the reaction rate between norbornene and tetrazine deratives. Three tetrazine building blocks were synthesized with substituents with decreased electron donating character, including 3-methyl and 6-phenyl (TZ1), 3-methylidene and 6-phenyl (TZ2) and 3-hydrogen and 6-phenyl (TZ3).[33] The norbornene and various tetrazines derivatives were then functionalized on 4-arm PEG star polymers to obtain hydrogels with macroporous structures of various size and porosity, mechanical properties and gelation kinetics. To examine the use of the IEDDA reaction pairs of various rates and their formed microporous structures in 3D cell culture, human primary chondrocytes that deposit large quantities of extracellular matrix were used reading out cell viability and glycosaminoglycan (GAGs) production.

5.3 Results and Discussion

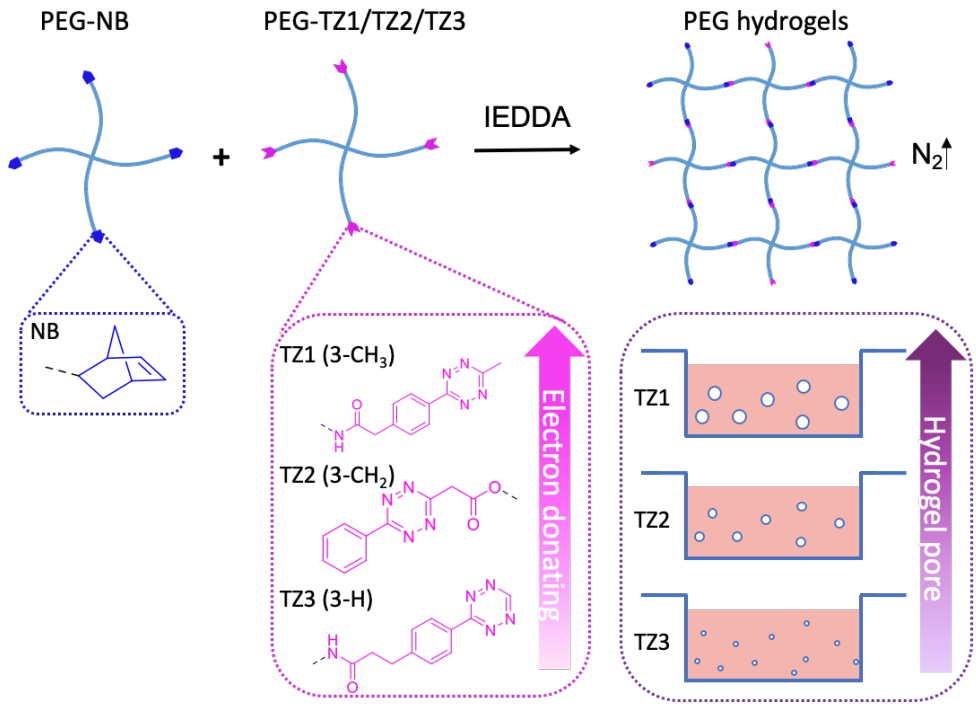

Scheme 5.1. Scheme of the IEDDA-bioconjugation reaction on PEG macromonomers and macropore formation in Tz-Nb-based PEG hydrogels with tetrazines bearing substituents of varying electron donating character. Mixing of PEG macromolecules **PEG-NB** and **PEG-TZ1/TZ2/TZ3** yields PEG hydrogels through cross-linking of the reactive groups and nitrogen gas is produced and captured in the hydrogels during the gelation process providing macropores of different size.

PEG macromonomer synthesis. A library of tetrazines with varied electron donating substituents were synthesized to screen their reactivity with norbornene by the IEDDA reaction on PEG macromonomers.[33–35] However, due to the limited design space for tetrazines that can react quickly with *trans*-cyclooctene, norbornene was selected as the dienophile, due to its availability and moderate reactivity in comparison to the highly reactive *trans*-cyclooctene.[24] The conventional synthesis of tetrazines starts by reacting aromatic or aliphatic nitriles with hydrazine to obtain the dihydrotetrazine as

an intermediate product, followed by an oxidation process to arrive to the final product. To improve the yield, catalysts such as sulphur, *N*-acetylcysteine, nickel and zinc triflates are used and more recently, a one-pot synthesis of tetrazines was also reported.[36,37] Based on the one-pot synthesis method, we successfully synthesized three tetrazines derivatives that have different electron donating and electron withdrawing substituents on positions 3 and 6 of the tetrazine ring (**TZ1**, **TZ2**, **TZ3**), with comparable yields that range from 27% to 45%. The generated carboxylic acid groups on the tetrazine and norbornene rings were used for further coupling onto hydroxy terminated PEG macromonomers through Steglich esterification or on amine-terminated PEG macromonomers by amide bond formation, resulting in yields of 70-80%. Tetrazine- (**PEG-TZ1**/**TZ2**/**TZ3**) and norbornene-functionalized 4-arm PEG macromonomers (**PEG-NB**) were obtained by precipitation in cold diethyl ether and dialyzed against water with a high degree of end-functionalization (**PEG-NB** ca. 90%; **PEG-TZ1** ca. 75%; **PEG-TZ2** ca. 90%; **PEG-TZ3** ca. 90%). Detailed synthetic procedures can be found in the Supporting Information.

PEG hydrogel preparation and characterization. Hydrogel formation based on the Tz-Nb crosslinks and their gelation time and stiffness were first examined by gel inversion and rheological measurements. PEG macromonomers **PEG-TZ** and **PEG-NB** were first dissolved in PBS (pH 7.4) or DMEM independently preparing stock solutions at various concentrations prior to mixing of the macromonomers in an equimolar ratio. Free standing and transparent hydrogels with gas bubbles of different sizes were observed by eye through a gel inversion test providing evidence for occurrence of the IEDDA reaction between the Tz and Nb groups (Figure S5.1). Oscillatory rheology was used to further quantify the mechanical properties and kinetics of gelation using equimolar precursor solutions prepared with final PEG macromonomer concentrations at 4 and 8 mM, respectively. Time sweep measurements provided insight into the gelation time through assessing the critical gelation point where G’ > G’’. Whereas Tz1-Nb-based PEG

hydrogels with a total PEG macromonomer concentration of 4 mM required ~ 4 h to reach the critical gelation point, Tz2-Nb and Tz3-Nb reaction pairs achieved gelation on the order of minutes, namely, 38 and 6 min, respectively (Figure 5.1). As expected, a longer gelation time for Tz1-Nb-based PEG hydrogels was demonstrated due to the increased electron donating effect of the substituents on the 3-position from TZ3 to TZ1 that decrease reactivity. Further increasing the total PEG macromonomer concentration to 8 mM, all hydrogels gelated within a shorter time, that is 40 min, 12 min and less than 1 min for Tz1-Nb, Tz2-Nb and Tz3-Nb-based PEG hydrogels, respectively. Similarly, Tz3-Nb-based hydrogels showed a 17-fold and 58-fold decreased critical gelation time in comparison to Tz1-Nb and Tz2-Nb-based hydrogels, respectively, demonstrating faster reaction kinetics of TZ3 with nobornene over TZ1 and TZ2. Through substitution of the tetrazine ring, control over the rate of hydrogel formation through Tz-Nb crosslinking was achieved. Because the gelation kinetics play an important role in cell encapsulation with fast gelation enabling a homogeneous cell distribution while slow gelation results in cell sedimentation, gelation times were further examined in the context of cell encapsulation in 3D. As an example, it was earlier demonstrated that reaction of unfunctionalized 4-arm PEG tetrazines and dinorbornene peptides (within minutes) resulted in hydrogels suitable for 3D cell encapsulation[28], whereas the slow reaction (over 5h) of furan and methylfuran gels resulted in high cell sedimentation.[38] Therefore, hydrogels based on TZ2 and TZ3 were further examined for their capacity to prepare gel phase materials for applications in 3D cell culture.

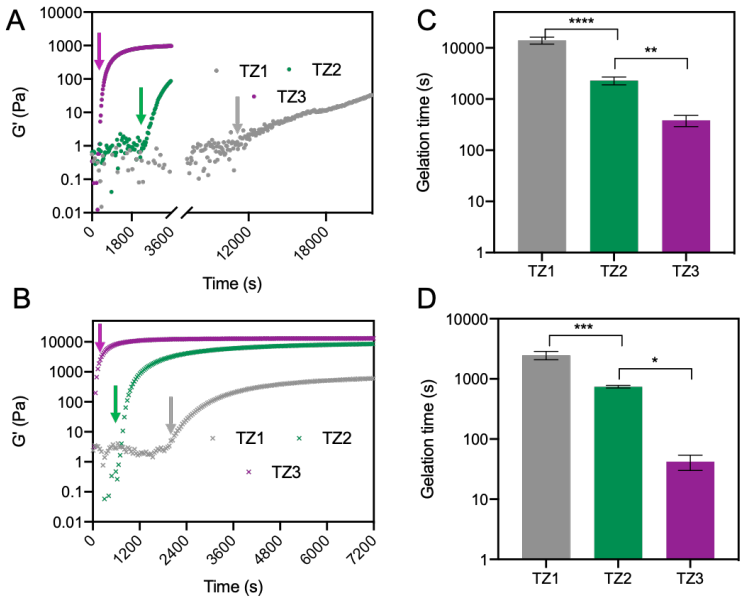

Figure 5.1. Tz-Nb-based PEG hydrogels that prepared with a norbornene/tetrazine molar ratios of 1:1. Time-sweep measurements of 4-arm PEG hydrogels with final PEG macromonomer concentrations of A) 4 mM and B) 8 mM. Arrows indicate the onset of gelation. Qualitative measurements of gelation time of hydrogels with PEG concentrations at C) 4 mM and D) 8 mM. The means and standard deviations are marked inside the graphs. (*P< 0.05, **P< 0.01, ***P< 0.001, ****P< 0.0001 one-way Anova)

From time sweep data, further mechanical information on the formed hydrogels was obtained from the measured plateau storage moduli (G'). The stiffness of Tz-Nb-based PEG hydrogels prepared from **PEG-TZ2** can be tuned from 1 Pa to 8.5 kPa by varying total PEG macromonomer concentrations from 2 mM to 8 mM, whereas for **PEG-TZ3** this range was higher in G' from 1 Pa to 12 kPa (Figure 5.2A). While, the case of Tz1-Nb-based PEG hydrogels displayed much lower storage moduli, showing a maxmium value at 1 kPa even with highest concentration of PEG macromonomer (16 mM), demonstrating the necessity of a faster reaction and gelation to engineer materials with higher mechanical properties (Figure S5.4). An amplitude sweep

experiment was performed from 0.1% to 1000% strain to determine linear viscoelastic (LVE) region of the materials. The end of the linear regime for the Tz2-Nb and Tz3-Nb-based hydrogels were at 300% and 127% with total PEG concentrations at 4 mM, and that were 99% and 123% with 8 mM PEG macromonomer concentration, respectively, after which permanent deformation occurred (Figure S5.4). Frequency sweep data shows that G' was significantly greater than G'' over an order of magnitude confirming the formation of elastic hydrogels (Figure S5.3).

To gain insight into the extent of crosslinking and stability of the hydrogel network, the equilibrium swelling ratio was determined for the Tz-Nb-based PEG hydrogels. The prepared hydrogels were incubated at 37˚C with PBS or DMEM medium and the weight of the hydrogels were measured at different time points. In the presence of PBS, whereas hydrogels based on TZ2 and TZ3 displayed stable weight ratios during the whole incubation, there was an 13% increase in the weight of the TZ1-based hydrogels after 15-day incubation with PBS (Figure 5.2B). This relatively higher swelling ratio (>1.14) of the Tz1-Nb-based hydrogel indicated a fraction of uncrosslinked polymer network that is consistent with a lower degree of functionalization of TZ1 on the PEG polymer in comparison to that of TZ2 and TZ3, that were 75% for TZ1 and over 90% for TZ2 and TZ3. In the case of DMEM, Tz2-Nb-based PEG hydrogels swelled slightly with a ratio of 4% during first two days and then showed clear decrease in swelling on day 3 and stabilized over the remainder of the experiment. Hydrogels based on TZ1 exhibited a decreased swelling ratios that end with 0.93 while TZ3-based hydrogel showed slightly incresed swelling behavior (1.07) (Figure S5.2). Still, neither hydrogels showed changes over the whole incubation period (15 days), demonstrating their stability during incubation with both PBS and DMEM, further supporting their use as scaffolds for 3D cell culture.

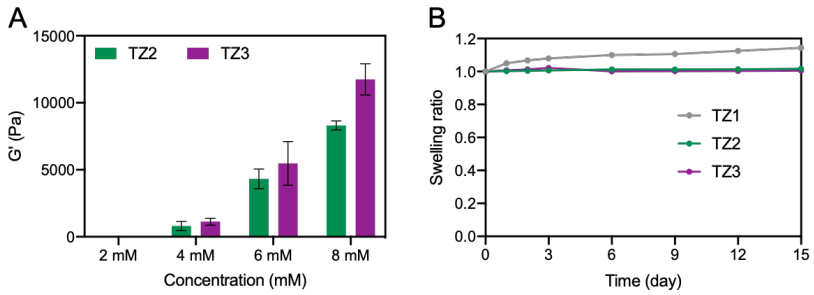

Figure 5.2 A) Averaged storage moduli (G') of Tz-Nb-based PEG hydrogels that were prepared in PBS and collected at 37 ± 0.2˚C by a time-sweep measurement with a fixed frequency of 1 Hz and strain of 0.05%. (N = 3) B) Swelling ratios of NB/TZ-based PEG hydrogels were measured over a period of 15-day incubation with PBS at 37˚C.

Macroscale pore measurement. During the IEDDA cycloaddition reaction between NB/TZ-based PEG macromonomers, nitrogen gas is released. According to the calculation, over 224 mg L^{-1} would be released when preparing Tz-Nb-based PEG hydrogels from 4 to 10 mM. This gas amount is far more than the solubility of nitrogen gas in water that is known as 15 mg L^{-1}. Therefore, the supersaturated nitrogen gas in the hydrogel results in the formation of bubbles. Owing to the different density between gas and liquid phase, bubbles usually move upwards and grow into larger new ones through coalescence. As this process can be influenced by the viscosity of the liquids they are prepared in by modulating bubble coalescence,[39,40] the use of hydrogelating materials based starting from synthetic polymer solutions can steer this process. Therefore, in the following experiment, we aimed to quantitatively assess the formed the macropore diameters to understand the connection between gelation rate and pore formation. Fluorescent RGD peptide sequences (NB-GGKGGGRGDS) containing a norbornene on the N-terminus and FITC label on the lysine side-chain were designed and coupled to Tz-Nb PEG hydrogels to visualize their formation. Because the fluorescent moiety is coupled to the forming polymer network, the resulting macropores were anticipated to appear as regions lacking fluorescence by confocal microscopy.

To probe the effect of the IEDDA gelation rate on macropore size, both slow and fast gelating hydorgels consisting of Tz2 and Tz3-based PEG macromonomers were prepared. Soft (1 kPa) and stiff (12 kPa) hydrogels by varying total polymer concentration with 4 and 8/10 mM for each Tz-Nb-based PEG hydrogel were obtained. The fluorescent hydrogels were imaged through taking z-stacks by confocal microscopy and the gas bubbles as indicated by the black spaces were measured in Fiji, as seen from Figure 5.3A and Figure S5.5. Pores were clearly formed and were distributed separately within the fluorescent hydrogels, confirming that the gelation process stopped the bubbles from coalescing. Size distributions of pore diameters were relatively broad ranging from 100 μm to 700 μm. A clear fraction of smaller size bubbles (< 300 μm) was observed in the most rapid hydrogel Tz3-Nb pointing to the importance of reaction rate on bubble formation (Figure 5.3B). Moreover, smaller pore diameters in Tz3-Nb PEG hydrogels having a total PEG concentration at 8 mM (268 ± 94 μm) were obtained over that of Tz2-Nb PEG hydrogels (382 ± 99 μm). Similarly, with a lower overall polymer concentration, hydrogels formed from TZ3 displayed significantly smaller bubbles (339 ± 135 μm) than gels consisting of TZ2 (417 ± 86 μm) (Figure 5.3C), demonstrating that faster gelation process resulted in hydrogels with smaller macropores and slower gelation resulted in larger macropores. Taken together, a control over hydrogel pore size can be achieved by tuning the rate of reaction through substitution of the tetrazine rings with electron donating substituents on the positions 3 or 6 with unsubstituted tetrazines reacting with norbornenes more rapidly than those substituted with methylenes on the 3-position to form smaller pores. With this tunable handle to control the pore size, the hydrogel porosity can also been tuned. And other parameters in terms of pore densities and their effect on cell behaviour can be explored in further study.

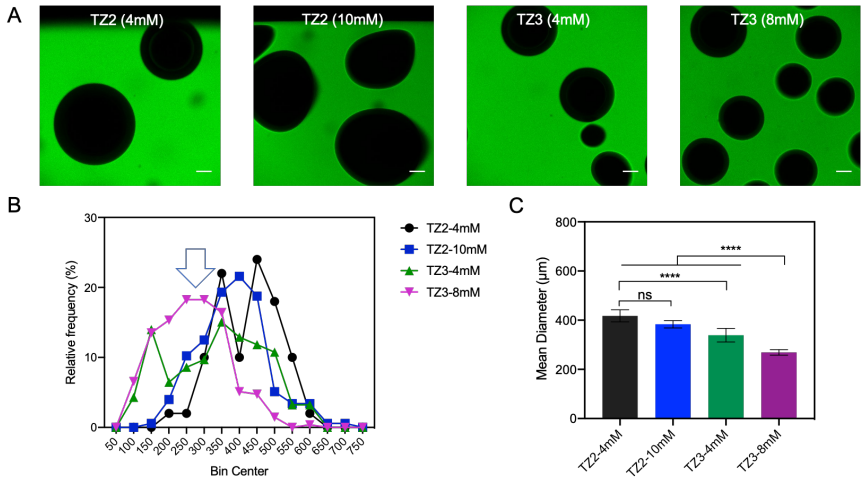

Figure 5.3. A) Representative images of FITC-labelled Tz-Nb-based PEG hydrogels prepared from **PEG-NB** and **PEG-TZ2/TZ3** polymers (hydrogels, *green;* pores*, black spaces*). Scale bar 100 µm. B) Size distribution and C) Mean diameter ± 95% confidence intervals from quantitative analysis of macropore diameters that formed in FITC-labelled PEG hydrogels. (****P< 0.0001 one-way Anova)

Primary chondrocytes culture within PEG hydrogel. In previous reports, it was demonstrated that the crosslinking between dinorbornene peptides and a Tz-functionalized PEG polymer can be used for 3D cell culture.[28,29] These results motivated us to explore potential of the Tz-Nb PEG hydrogels of various reactivities in the current work for 3D cell culture applications. We are particularly interested in the culture of primary chondrocytes because they play in important role in cartilage homeostasis, with their imbalance resulting in degenerative disease. Earlier reports have demonstrated that porous hydrogels with pore sizes between 250 to 500 µm have been demonstrated to be beneficial for chondrocyte growth and matrix production of collagen and proteoglycans through providing extra space for the newly formed biopolymers.[41,42] We thus became interested in evaluating the rate of the Tz-Nb reaction on 3D cell seeding and the effect of the formed pore sizes prepared by the in situ forming gas reaction on primary chondrocyte matrix production.

Primary chondrocytes were cultured for two passages after isolation from healthy cartilage and seeded into PEG hydrogels with a cell density of 2 x 10^6 cells/mL and cultured overnight followed by a 4-day differentiation process. LIVE/DEAD staining of chondrocytes were performed on day 2 and 5 of the culture to gain information on cell viability in the synthetic polymer matrices. From the z-stack images, Tz2-Nb-based PEG hydrogels showed cell sedimentation owing to the slower gelation process compared with those containing Tz3-Nb crosslinks. Still, the cells were largely viable in the matrices as shown by their green-staining for all tested conditions, with cell viabilities ranging from 80-97% that were calculated by counting live and dead cell populations after the LIVE/DEAD staining (Figure 5.4). Moreover, after 5 days of cell culture, the macropores stayed visible in the hydrogels demonstrating the stability of macropores after bubble formation and facilitating nutrition exchange.

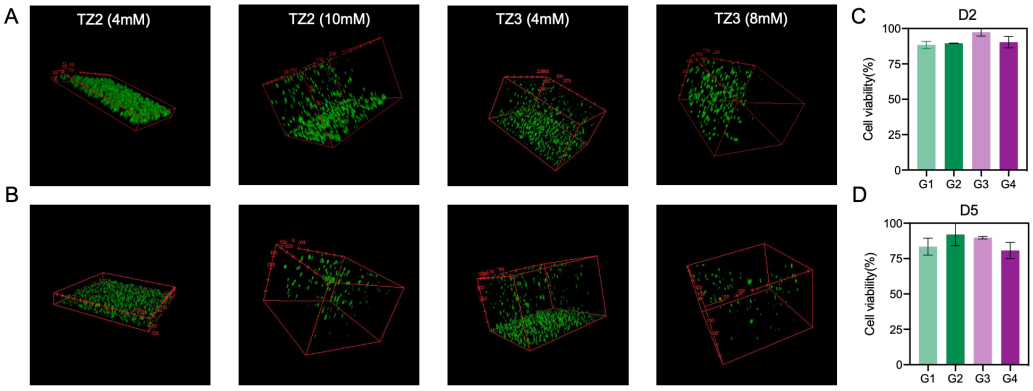

Figure 5.4. Cytocompatibility of Tz-Nb-based PEG hydrogels (NB:TZ molar ratio 1:1). Representative z-stack images of cells cultured in the hydrogels at A) day 2 and B) day 5. Cells were stained with calcein AM (viable cells, *green*) and propidium iodide (PI) (dead cells, *red*). Scale bar = 100 µm. Quantification of cell viability by cell counting in ImageJ after culture C) day 2 and D) day 5. Error bars represent standard deviations of the data.

Chondrocytes actively secrete extracellular matrix consisting of collagen (mainly type II) proteins, proteoglycans and hyaluronan. To detect matrix secretion, the histochemical stain Alcian blue was used to detect and quantify glycosaminoglycans

(GAGs) colourimetrically through their dark blue colour.[43,44] When the chondrocytes are assembled as pellets, extracellular matrix production is observed 2-3 days after differentiation. In this study, chondrocytes were encapsulated within hydrogels and fixed after differentiation on day 4 and stained with Alcian blue. Cells cultured in soft hydrogels (G' = 1 kPa) showed a dark, dense blue "membrane" around the cells on staining (indicated by the white arrows in Figure 5.5). In contrast, in stiff Tz-Nb-based PEG hydrogels (G' = 12 kPa), blue stained cells were hardly found suggesting that primary chondrocytes prefer a softer environment to facilitate GAGs secretion.

Matrix cues such as those of a biochemical and biophysical nature have been reported to affect ECM production and redifferentiation of chondrocytes.[45,46] In 3D culture systems in a stiff microenvironment, primary chondrocytes usually show a spherical morphology and display increased matrix production, for example, in fibrin and GelMA hydrogels with Young's moduli around 30 kPa.[43,47] In the current study, the chondrocytes showed matrix production in relatively softer hydrogels and in areas where cells tended to aggregate. The observed result could be due to the close cell-cell contacts that are made.[48] While the correlation between hydrogel pore size and chondrocyte matrix production needs to be explored more thoroughly, these preliminary results suggest that primary chondrocytes survive and secrete GAGs in Tz-Nb-based PEG hydrogels and further demonstrate their potential for further use in biomedical applications.

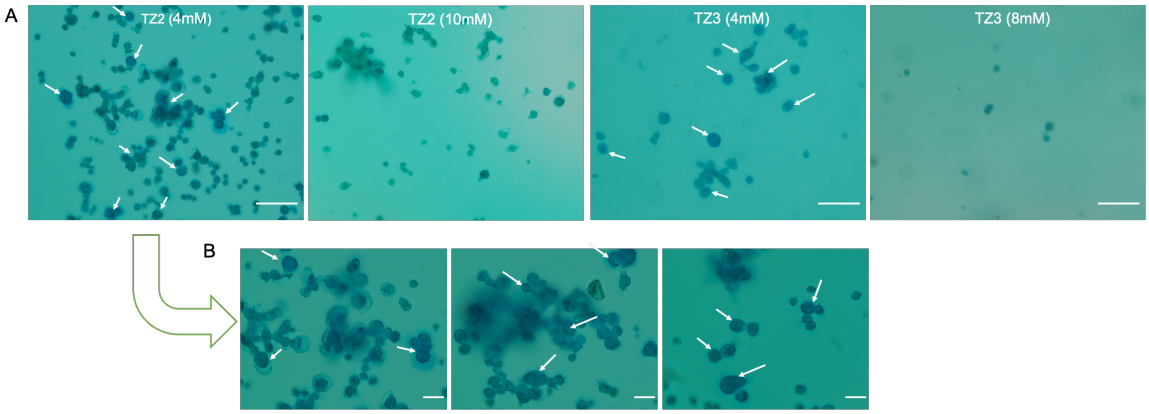

Figure 5.5. A) Images of Alcian blue stained primary chondrocytes in Tz-Nb-based PEG hydrogels under a 20x objective on an Olympus microscope. B) Representative images of Alcian blue stained primary chondrocytes in Tz2-Nb-based PEG hydrogels with a total polymer concentration of 4 mM. Imaged were collected under a 40x objective. Arrows highlight dark blue-stained extracellular matrix of chondrocytes in hydrogels that are mechanically soft (G' 1 kPa). Scale bar: 100 µm.

5.4 Conclusions

In summary, we hereby show a control over the pores size of a PEG-based hydrogels through controlling the rate of the tetrazine-norbornene reaction. Three tetrazines that have varied electron donating substituents were successfully synthesized and coupled onto multi-arm PEG polymers, respectively. The PEG-TZ macromonomers were further crosslinked with Nb-functionalized multi-arm PEG polymers through the IEDDA reaction, forming elastic hydrogels of varying stiffness. The nitrogen gas produced during the IEDDA reaction on the polymers enable microporous hydrogel formation. The gelation kinetics and pore sizes and porosity were observed to depend highly on the IEDDA reaction rates and PEG macromonomer concentrations, with higher reaction rates and polymer concentrations yielding faster gelation. The fastest gelation behaviour was observed in TZ3 that lacks electron donating substitution and is

consistent with its rapid crosslinking kinetics. Rheological experiments demonstrated that these Tz-Nb-based PEG hydrogels can be prepared with storage moduli ranging from 0.7 kPa to 12 kPa through increasing concentration and the reaction rate of the components by tetrazine selection. The faster gelation of the Tz3-Nb PEG hydrogel minimized the bubble coalescence during bubble formation, resulting in the formation of hydrogels with a significantly smaller pores with an average diameter of 268 $\pm$ 94 µm was obtained in comparison to Tz2-Nb-based PEG hydrogels (382 $\pm$ 99 µm). All the Tz-Nb-based PEG hydrogels were demonstrated to be stable in presence of PBS and DMEM medium as shown in swelling tests, despite a fraction of uncrosslinked PEG macromonomer in the Tz1-Nb-based PEG hydrogel. The high stability of the hydrogels further allowed them to be used as a synthetic matrix for 3D cell culture. 3D encapsulated primary chondrocytes in soft Tz-Nb-based PEG hydrogels displayed high viability and notable changes in cartilage matrix secretion, demonstrating their potential application in cartilage tissue engineering, though further quantitative analysis is necessary to gain conclusion about effect of hydrogel pore size on matrix production. In conclusion, we showed a control over hydrogel pore size and porosity can be achieved by tuning the reaction rate of the IEDDA components by substituting tetrazine rings to control over physicochemical aspects matrix properties for *in vitro* cell culture applications in 3D.

5.5 References

[1] F. Edalat, I. Sheu, S. Manoucheri, A. Khademhosseini, *Curr. Opin. Biotechnol.* **2012**, *23*, 820.

[2] C. Bonnans, J. Chou, Z. Werb, *Nat. Rev. Mol. Cell Biol.* **2014**, *15*, 786.

[3] G. Huang, F. Li, X. Zhao, Y. Ma, Y. Li, M. Lin, G. Jin, T. J. Lu, G. M. Genin, F. Xu, *Chem. Rev.* **2017**, *117*, 12764.

[4] J. Nicolas, S. Magli, L. Rabbachin, S. Sampaolesi, F. Nicotra, L. Russo, *Biomacromolecules* **2020**, *21*, 1968.

[5] K. M. Schultz, K. A. Kyburz, K. S. Anseth, *Proc. Natl. Acad. Sci. U. S. A.* **2015**, *112*, E3757.

[6] X. Li, Y. Chen, N. Kawazoe, G. Chen, *J. Mater. Chem. B* **2017**, *5*, 5753.

[7] N. Huebsch, E. Lippens, K. Lee, M. Mehta, S. T. Koshy, M. C. Darnell, R. M. Desai, C. M. Madl, M. Xu, X. Zhao, O. Chaudhuri, C. Verbeke, W. S. Kim, K. Alim, A. Mammoto, D. E. Ingber, G. N. Duda, D. J. Mooney, *Nat. Mater.* **2015**, *14*, 1269.

[8] X. Xie, X. Li, J. Lei, X. Zhao, Y. Lyu, C. Mu, D. Li, L. Ge, Y. Xu, *Mater. Sci. Eng. C* **2020**, *116*, 111165.

[9] T. Tokatlian, C. Cam, T. Segura, *Adv. Healthc. Mater.* **2015**, *4*, 1084.

[10] V. Zubillaga, A. Alonso-varona, S. C. M. Fernandes, A. M. Salaberria, T. Palomares, *Int. J. Mol. Sci.* **2020**, *21*, 1.

[11] B. Conrad, L. H. Han, F. Yang, *Tissue Eng. - Part A* **2018**, *24*, 1631.

[12] S. S. Ng, K. Saeb-Parsy, S. J. I. Blackford, J. M. Segal, M. P. Serra, M. Horcas-Lopez, D. Y. No, S. Mastoridis, W. Jassem, C. W. Frank, N. J. Cho, H. Nakauchi, J. S. Glenn, S. T. Rashid, *Biomaterials* **2018**, *182*, 299.

[13] I. Bružauskaitė, D. Bironaitė, E. Bagdonas, E. Bernotienė, *Cytotechnology* **2016**, *68*, 355.

[14] B. Podhorská, M. Vetrík, E. Chylíková-Krumbholcová, L. Kománková, N. R. Banafshehvaragh, M. Šlouf, M. Dušková-Smrčková, O. Janoušková, *Appl. Sci.* **2020**, *10*, 5.

[15] B. R. Thompson, T. S. Horozov, S. D. Stoyanov, V. N. Paunov, *J. Mater. Chem. A* **2019**, *7*, 8030.

[16] K. J. De France, F. Xu, T. Hoare, *Adv. Healthc. Mater.* **2018**, *7*, 1.

[17] O. D. Velev, E. W. Kaler, *Adv. Mater.* **2000**, *12*, 531.

[18] N. Adnan, S. Ghazali, S. S. Jamari, *Mater. Today Proc.* **2019**, *17*, 995.

[19] W. T. Han, T. Jang, S. Chen, L. S. H. Chong, H. Do Jung, J. Song, *Biomater. Sci.* **2020**, *8*, 450.

[20] W. Hu, Z. Wang, Y. Xiao, S. Zhang, J. Wang, *Biomater. Sci.* **2019**, *7*, 843.

[21] N. K. Devaraj, *ACS Cent. Sci.* **2018**, *4*, 952.

[22] Y. Liu, M. Liu, Y. Zhang, Y. Cao, R. Pei, *New J. Chem.* **2020**, *44*, 11420.

[23] A. C. Knall, C. Slugovc, *Chem. Soc. Rev.* **2013**, *42*, 5131.

[24] B. L. Oliveira, Z. Guo, G. J. L. Bernardes, *Chem. Soc. Rev.* **2017**, *46*, 4895.

[25] L. Bian, M. Guvendiren, R. L. Mauck, J. A. Burdick, *Proc. Natl. Acad. Sci. U. S. A.* **2013**, *110*, 10117.

[26] B. Yang, S. Tang, C. Ma, S. T. Li, G. C. Shao, B. Dang, W. F. DeGrado, M. Q. Dong, P. G. Wang, S. Ding, L. Wang, *Nat. Commun.* **2017**, *8*, 1.

[27] N. Gjorevski, N. Sachs, A. Manfrin, S. Giger, M. E. Bragina, P. Ordóñez-Morán, H. Clevers, M. P. Lutolf, *Nature* **2016**, *539*, 560.

[28] D. L. Alge, M. A. Azagarsamy, D. F. Donohue, K. S. Anseth, *Biomacromolecules* **2013**, *14*, 949.

[29] V. X. Truong, M. P. Ablett, S. M. Richardson, J. A. Hoyland, A. P. Dove, *J. Am. Chem. Soc.* **2015**, *137*, 1618.

[30] R. M. Desai, S. T. Koshy, S. A. Hilderbrand, D. J. Mooney, N. S. Joshi, *Biomaterials* **2015**, *50*, 30.

[31] V. Delplace, P. E. B. Nickerson, A. Ortin-Martinez, A. E. G. Baker, V. A. Wallace, M. S. Shoichet, *Adv. Funct. Mater.* **2020**, *30*, 1.

[32] D. S. B. Anugrah, M. P. Patil, X. Li, C. M. Q. Le, K. Ramesh, G. D. Kim, K. Hyun, K. T. Lim, *Express Polym. Lett.* **2020**, *14*, 248.

[33] M. R. Karver, R. Weissleder, S. A. Hilderbrand, *Bioconjug. Chem.* **2011**, *22*, 2263.

[34] J. Schoch, M. Wiessler, A. Jäschke, *J. Am. Chem. Soc.* **2010**, *132*, 8846.

[35] K. Lang, L. Davis, J. Torres-Kolbus, C. Chou, A. Deiters, J. W. Chin, *Nat. Chem.* **2012**, *4*, 298.

[36] W. Mao, W. Shi, J. Li, D. Su, X. Wang, L. Zhang, L. Pan, X. Wu, H. Wu, *Angew. Chemie - Int. Ed.* **2019**, *58*, 1106.

[37] J. Yang, M. R. Karver, W. Li, S. Sahu, N. K. Devaraj, *Angew. Chemie - Int. Ed.* **2012**, *51*, 5222.

[38] C. M. Madl, S. C. Heilshorn, *Chem. Mater.* **2019**, *31*, 8035.

[39] K. Yamada, H. Emori, K. Nakazawa, *Earth, Planets Sp.* **2008**, *60*, 661.

[40] A. Barbetta, A. Gumiero, R. Pecci, R. Bedini, M. Dentini, *Biomacromolecules* **2009**, *10*, 3188.

[41] H. Akkiraju, A. Nohe, *J. Dev. Biol.* **2015**, *3*, 177.

[42] S. M. Lien, L. Y. Ko, T. J. Huang, *Acta Biomater.* **2009**, *5*, 670.

[43] B. Bachmann, S. Spitz, B. Schädl, A. H. Teuschl, H. Redl, S. Nürnberger, P. Ertl, *Front. Bioeng. Biotechnol.* **2020**, *8*, 1.

[44] L. A. Smith Callahan, A. M. Ganios, E. P. Childers, S. D. Weiner, M. L. Becker, *Acta Biomater.* **2013**, *9*, 6095.

[45] W. Wei, Y. Ma, X. Yao, W. Zhou, X. Wang, C. Li, J. Lin, Q. He, S. Leptihn, H. Ouyang, *Bioact. Mater.* **2021**, *6*, 998.

[46] H. J. Lee, Y. Seo, H. S. Kim, J. W. Lee, K. Y. Lee, *ACS Omega* **2020**, *5*, 15567.

[47] X. Li, S. Chen, J. Li, X. Wang, J. Zhang, N. Kawazoe, G. Chen, *Polymers (Basel).* **2016**, *8*, 269.

[48] TS. de Windt, DB. Saris, IC. Slaper-Cortenbach, MH. van Rijen, D. Gawlitta, LB. Creemers, RA. de Weger, WJ. Dhert, LA.R. Vonk. J. Siman. *Tissue Eng Part A.* **2015**, *21*, 2536.

5.6 Supporting information

5.6.1 Materials

Tetra-arm hydroxy-terminated PEG (Mw 10kDa) was purchased from Creative PEGWorks and tetra-arm amine-terminated PEG (Mw 10kDa) was from Jenkem Technology. Deuterated dimethyl sulfoxide (DMSO-d_6) and chloroform ($CDCl_3$) were purchased from Eurisotop. All other chemicals and reagents for synthesis were purchased from Sigma Aldrich and used without further purification. Dulbecco's Modified Eagles Medium (DMEM) and fetal bovine serum (FBS), penicillin, streptomycin and trypsin-EDTA were from Gibco. Human basic fibroblast growth factor (hFGF) and human transforming growth factor β1 (hTGF-β1) were purchased from PeproTech. Dulbecco's Phosphate Buffered Saline (DPBS), calcein AM (AM = acetoxymethyl), propidium iodide (PI) and alcian-blue staining solution were obtained from Sigma-Aldrich.

5.6.2 Instruments

^{1}H-NMR and ^{13}C-NMR spectra were acquired on a Bruker DMX-400 and Bruker DPX-300 MHz at 298K. LC-MS analysis was performed on a TSQ Quantum Access MAX system equipped with a Gemini 3 µm C18 110 Å 50×4.60 mm column (UV detection at 214 nm and 254 nm, mass detection range: 160 to 2000 (Da)). The mobile phase consisted of a gradient of 10-90% of H_2O-ACN with 0.1% trifluoroacetic acid (TFA) over 13.5 minutes. HPLC purification of peptides was executed on a C18 column with a gradient of 1-10% ACN/H_2O over 15 min at a flow rate of 12 mL/min. High resolution mass spectra (HR-MS) were collected on a Thermo Fisher LTQ Orbitrap mass spectrometer equipped with an electrospray ion source in positive mode. Samples were prepared in a mixture solvent (DMSO-H_2O-ACN, 1 mg/mL) and injected directly. Oscillatory rheology experiments were performed on a Discovery HR-2 hybrid rheometer using a cone-plate

geometry (20 mm, 1.995°) at 37 ± 0.2 °C with a peltier-based temperature controller and solvent trap. Confocal fluorescent images were acquired on Leica TCS SP8 confocal laser scanning microscope equipped with a 10× air objective. Images were processed using the Fiji Image J software. Alcian-blue staining images were collected on an Olympus microscopy equipped with 20× and 40x air objectives.

5.6.3 Synthesis and experimental details

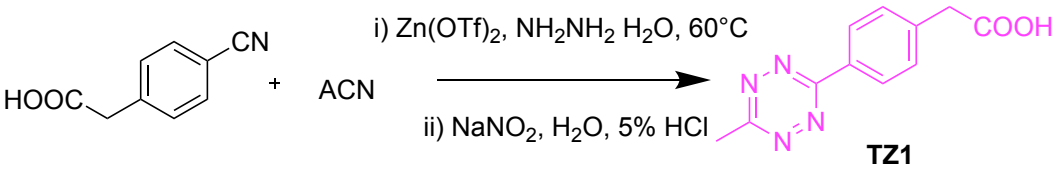

Scheme S5.1. Synthesis route of **TZ1**[1]

Synthesis of TZ1. 4-Cyanophenylacetic acid (1.15 g, 7.13 mmol), $Zn(OTf)_2$ (1.30 g, 3.57 mmol) and acetonitrile (3.60 mL, 68.93 mmol) were mixed under N_2 (50 mL). A solution of hydrazine hydrate (16.80 mL, 346.33 mmol) was added dropwise. The reaction mixture was stirred overnight at 60˚C. After that, the obtained orange-yellow solution was cooled to room temperature, followed by the addition of $NaNO_2$ (9.60 g, 139.15 mmol) in H_2O (50 mL). Next, the reaction mixture was acidified to pH=1 by the dropwise addition of HCl (4M), and extracted with EtOAc (100 mL x 3). The combined organic layers were washed with brine (100 mL x 3), dried over anhydrous Na_2SO_4 and concentrated in vacuum overnight to obtain the product as a pink solid. Yield: 45.0%, 0.74 g. ^{1}H-NMR (DMSO-d_6, 400 MHz): 8.43-8.41 (d, 2H), 7.56-7.54 (d, 2H), 3.73 (s, 2H), 2.99 (s, 3H). ^{13}C-NMR (DMSO-d_6, 100 MHz): 172.29, 167.12, 163.22, 139.80, 130.58, 130.30, 127.35, 40.55, 20.85. HR-MS: $[M+H]^+$: calcd: 233.1033 (protonated), found: 233.1033.

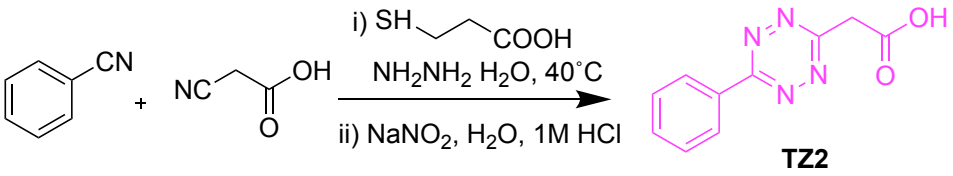

TZ2

Scheme S5.2. Synthesis route of **TZ2**[2]

Synthesis of TZ2. Benzonitrile (510 µL, 4.95 mmol), 2-cyanoacetic acid (3.40 g, 39.97 mmol) and 3-mercaptopropionic acid (87 µL,0.99 mmol) were cooled to 0°C and mixed under N_2. To this mixture, hydrazine monohydrate (3.8 mL, 78.33 mmol) was added slowly and the resulting mixture was stirred at 40°C for 20 h. After that, cold aqueous solution of sodium nitrite (5.23 g, 75.80 mmol) was added and left to stir at room temperature for 30 min. The crude reaction mixture was adjusted to pH ~3 with the slow addition of ice-cold 1M HCl. (Caution: the addition of HCl resulted in formation of toxic nitrogen oxide gas) After stirring for 30 min, the crude was extracted with DCM (100 mL x 5). The organic layers were combined, dried over Na_2SO_4, and concentrated by rotary evaporation. Lastly, the crude was purified by flash column chromatography on silica gel with 10% EtOAC in DCM. The purified fractions were collected, evaporated and dried in vacuum oven overnight to obtain **TZ2** as a pink solid.

Yield: 27.1%, 0.29 g. ^{1}H-NMR (DMSO-d_6, 400 MHz): 8.52-8.46 (m, 2H), 7.75-7.65 (m, 3H), 4.41, 3.00 (s, 2H). ^{13}C-NMR (DMSO-d_6, 100 MHz): 169.94, 165.11, 163.63, 132.84, 131.55, 129.56, 127.73, 40.72. HR-MS: $[M+H]^+$: calcd: 217.0720, found: 217.0720.

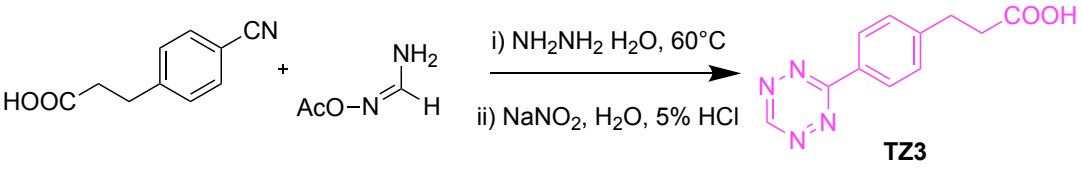

TZ3

Scheme S5.3. Synthesis route of **TZ3**[3,4]

Synthesis of TZ3. A mixture of 3-(4-Cyanophenyl)propionic acid (1.10 g, 6.28 mmol) and formamidine acetate salt (4.12 g, 39.57 mmol) was cooled to 0°C under N_2.

Hydrazine monohydrate (8.0 mL, 164.92 mmol) was added slowly and the resulting mixture was warmed to 60°C and stirred for 3h. Once cooled, the reaction mixture was further stirred overnight and then neutralized to pH 7 with 5% aqueous HCl. Afterwards, a cold aqueous solution of sodium nitrite (2.76 g, 40.01 mmol) was added and stirred for another 30 min. Then, an ice-cold 5% aqueous HCl solution was added slowly until the solution reached pH ~3. (Caution: the addition of HCl resulted in formation of toxic nitrogen oxide gas) After leaving the reaction mixture to stir for another 30 min, the pink precipitate was collected by filtration, washed with 0.1% aqueous HCl and dried in vacuum to obtain **TZ3** a pink solid without further purification.

Yield: 33.8%, 0.49 g. ^{1}H-NMR (DMSO-d_6, 400 MHz): 10.55 (s, 1H), 8.42-8.39 (d, 2H), 7.54-7.52 (d, 2H), 2.96-2.93 (t, 2H), 2.64-2.60 (t, 2H). ^{13}C-NMR (DMSO-d_6, 100 MHz): 173.77, 165.61, 158.18, 146.54, 129.81, 129.61, 127.95, 34.82, 30.41. HR-MS: $[M+H]^+$: calcd: 233.1033 (protonated), found: 233.1033.

Synthesis of PEG-NB.[5] 5-norbornene-2-carboxcylic acid (600 µL, 4.43 mmol) and N,N'-dicyclohexylcarbodiimide (0.53 g, 4.64 mmol) were dissolved in dry DCM and reacted at room temperature for 30 min. In a separate reaction vessel, tetra-arm hydroxyl-terminated PEG (Mw 10 kDa) (2.00 g, 0.20 mmol) together with 4-(dimethylamino)pyridine (DMAP) (0.05 g, 0.44 mmol) and pyridine (0.33 mL, 4.10 mmol) were dissolved in dry DCM. Subsequently, the PEG solution was added dropwise into the activated norbornene solution and the reaction mixture was left to stir at room temperature for 24 h. The reaction crude was first filtered and the filtrate was precipitated from cold diethyl ether, washed, dissolved in DCM, and re-precipitated from cold diethyl ether. The obtained products after three rounds of precipitation were re-dissolved in water and lyophilized to obtain **PEG-NB** as a white solid. Yield:1.59 g, 79.5%. ^{1}H-NMR (400 MHz, 298K, $CDCl_3$): 6.20-5.92 (m, 2H), 4.25-4.15 (m, 2H), 3.81-3.40 (m, 224H). The degree of functionalization of the **NB** group was calculated to be 90% based on ^{1}H-NMR.

Synthesis of PEG-TZ1.[1] **TZ1** (0.19 g, 0.80 mmol), BOP (0.35 g, 0.80 mmol) and tetra-arm amine-terminated PEG (0.50 g, 0.05 mmol) were dissolved in a dry and N_2-purged flask with dry DMF. N,N-diisopropylethylamine (DIPEA) (0.56 mL, 3.21 mmol) was added and the reaction mixture were left stirring at room temperature over the weekend. After that, the DMF was removed by rotary evaporation and the obtained residue was dissolved in DCM (50 mL), and subsequently washed with NaH_2PO_4 (1M, 50 mL x 2) and brine (50 mL x 2). The organic layer was dried, concentrated and precipitated from cold diethyl ether. The obtained red solid was dissolved in DCM and precipitated from cold diethyl ether for another two rounds, after which the red solid was dissolved in water, dialyzed against water for 48 h and lyophilized to obtain **PEG-TZ1** as a pink solid. Yield: 0.38 g, 76.2%. ^{1}H-NMR (400 MHz, 298K, $CDCl_3$): 8.41-8.39 (m, 2H), 7.55-7.53 (m, 2H), 3.69-3.50 (m, 224H), 2.99 (s, 3H). The degree of functionalization of the **TZ1** group was calculated to be 75% based on ^{1}H-NMR.

Synthesis of PEG-TZ2. TZ2 (0.33 g, 1.54 mmol), N-(3-dimethylaminopropyl)-N'-ethylcarbodiimide hydrochloride (0.36 g, 1.87 mmol) and 4-(dimethylamino)pyridine (0.20 g, 1.61 mmol) were dissolved in a dry and N_2-purged flask with dry DCM and reacted for 10 min as solution one. In a separate reaction vessel, tetra-arm hydroxyl-terminated PEG (0.60 g, 0.06 mmol) was dissolved in dry DCM and added dropwise into solution one. The reaction mixture was left stirring at room temperature over the weekend. Afterwards, the reaction crude was first precipitated from cold diethyl ether. The obtained red solid was dissolved in DCM and the precipitated salts were filtered off. The filtrate was precipitated in cold diethyl ether, dissolved in DCM and re-precipitated from cold diethyl ether. The obtained products after three rounds of precipitation were dissolved in water, dialyzed against water for 48 h and lyophilized to obtain **PEG-TZ2** as a pink solid. Yield: 0.44 g, 73.3%. ^{1}H-NMR (400 MHz, 298K, DMSO-d_6): 8.52-8.50 (m, 2H), 7.74-7.67 (m, 3H), 4.54 (s, 2H), 4.26-4.24 (m, 2H), 3.68-3.48 (m, 224H). The degree of functionalization of the **TZ2** group was calculated to be 90% based on ^{1}H-NMR.

Synthesis of PEG-TZ3. TZ3 (0.14 g, 0.61 mmol), BOP (0.26 g, 0.59 mmol) and tetra-arm amine-terminated PEG (0.40 g, 0.04 mmol) were dissolved in a dry and N_2-purged flask with dry DMF. DIPEA (0.80 mL, 4.59 mmol) was added and the reaction mixture was left to stir at room temperature over the weekend. After that, DMF was removed by rotary evaporation and the obtained residue was dissolved in DCM (50 mL), and subsequently washed with NaH_2PO_4 (1M, 50 mL x 2) and brine (50 mL x 2). The organic layer was dried, concentrated and precipitated from cold diethyl ether. The obtained red solid was dissolved in DCM and precipitated from cold diethyl ether for another two rounds, after which the red solid was re-dissolved in water, dialyzed against water for 48 h and lyophilized to obtain **PEG-TZ3** as a pink solid. Yield:0.28 g, 70.5%. ^{1}H-NMR (400 MHz, 298K, CDCl3): 10.57 (s, 1H), 8.43-8.40 (m, 2H), 7.56-7.54 (m, 2H), 4.14-4.09 (m, 2H), 3.68-3.31 (m, 224H), 3.01-2.97 (m, 2H), 2.76-2.72 (m, 2H). The degree of functionalization of the **TZ3** group was calculated to be 90% based on ^{1}H-NMR.

Peptide synthesis. The RGD peptide (GGGRGDS) was synthesized on an automatic CEM peptide synthesizer on a 100 µmol scale as described in Chapter 2. Norborne functionalization was manually performed by on the resin. Briefly, the obtained resins (100 µmol) from peptide synthesizer were suspended in DMF (2 mL) for 15 min. 5-Norbornene-2-carboxylic acid (53.3 mg, 0.54 mmol) was coupled to the N-terminus of the peptide by incubation with HCTU (g, 0.50 mmol) and DIPEA (175 µL, 1.00 mmol) in DMF (4 mL) at room temperature for 1h. Afterwards, the norbornene-functionalized peptides (RGD-NB) were cleaved in a TFA solution containing 2.5% H_2O and 2.5% triisopropylsilane (TIPS) for 3h, and then precipitated from cold diethyl ether, dried, dissolved in water and purified by HPLC using a gradient 1-10% ACN/H_2O over 15 min. The product was concentrated by evaporation and lyophilized overnight to obtain a light yellowish solid. LC-MS: t =0.69 min, m/z $[M+H]^+$: calcd: 724.31, found: 724.47.

Another RGD peptide (GGKGGGRGDS) was synthesized on an automatic CEM peptide synthesizer on a 100 µmol scale and norbornene-functionalization was performed in

the same method as above. Afterwards, the obtained resins were washed with a Mtt-deprotection solution (DCM:TFA:TIPS 94/1/5 v/v/v) until the filtrate becomes colorless. Then, the resins were washed with DCM (5 mL x3) before reacting with 5(6)-carboxyfluorescein (193 mg, 0.51 mmol) in combination with HBTU (201 mg, 0.53 mmol) and DIPEA (60 µL, 0.34 mmol) in DMF (5 mL) on a shaker for 3h. The coupling was performed twice. When finished, the resins were washed with DMF (5 mL x 3) and DCM (5 mL x 3) and the peptides were cleaved in a TFA solution (2.5% H_2O, 2.5% TIPS) for 3h. The peptides were then precipitated in cold diethyl ether, dried, dissolved in water and purified by HPLC using a gradient 1-10% ACN/H_2O over 15 min. The product was concentrated by evaporation and lyophilized overnight to obtain a yellow solid (FITC-RGD). LC-MS: t =4.71 min, m/z $[M+H]^+$: calcd: 1324.50, found: 1325.47.

5.6.3 Hydrogel preparation

Hydrogels were prepared by separately dissolving PEG macromonomers in PBS (pH 7.4) and mixing in a molar ratio of 1:1. More specfically, a freshly prepared solution of **PEG-NB** (100 µL) was mixed with that of **PEG-TZ1**/**TZ2**/**TZ3** (100 µL), and vortexed for 10s to obtain a homogeneous solution with a final PEG macromonomer concentration from 2-16 mM. For gelation, the precursor solutions were left at 37˚C. Images were taken after a free-standing hydrogel was obtained.

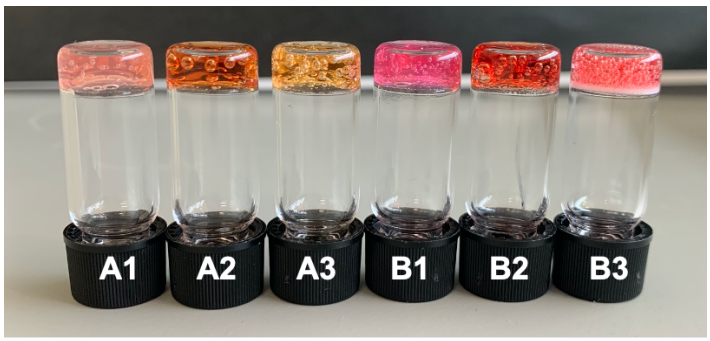

Figure S5.1. Gel inversion images of PEG hydrogels prepared from macromonomers **PEG-NB** and **PEG-TZ1**/**TZ2**/**TZ3** with a norbornene/tetrazine molar ratio of 1:1 in PBS (A,

pH 7.4) and DMEM medium (B), respectively. Numbers in the labels indicate the different tetrazine derivatives used for gel preparation.

5.6.4 Swelling measurements

Hydrogels (200 µL) were prepared according to gelation protocol described above and were allowed to stand at 37°C for 2h. After the gelation, the wet weight of these hydrogels was measured and denoted as W_0. Afterwards, PBS (pH7.4, 300 µL) or DMEM medium was added on top of hydrogel and incubated at 37˚C. At pre-determined time points, the supernatant solution was carefully removed and the wet weight of these hydrogels was measured and donoted as W_t. The swelling ratios over the time points were determined by the following equation: swelling ratio = W_t/W_0.

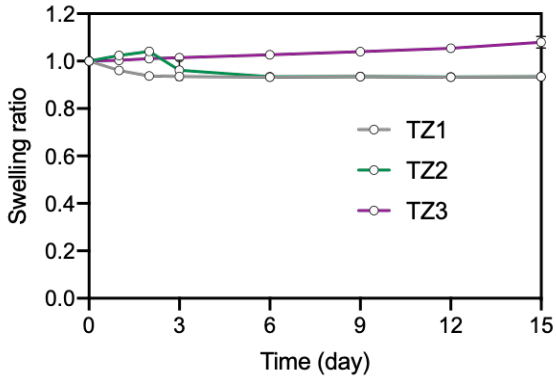

Figure S5.2. Swelling ratios of Tz-Nb-based PEG hydrogels in DMEM over a 15-day incubation period.

5.6.5 Oscillatory Rheology

Oscillatory rheology experiments were carried out on a Discovery HR-2 hybrid rheometer using parallel plate geometry (20 mm diameter) at 37 °C ± 0.2 °C with a Peltier-based temperature controller and a solvent trap. The prepared hydrogel (100 µL) was pipetted onto the bottom plate and the geometry was lowered to a gap distance

of 300 µm. Time sweep measurements were executed at a frequency of 1.0 Hz and strain of 0.05% and frequency sweeps were conducted from 0.01−10 Hz with 0.05% strain. Subsequently, amplitude sweeps were carried out with strains ranging from 0.1% to 2000% and a fixed frequency of 1.0 Hz.

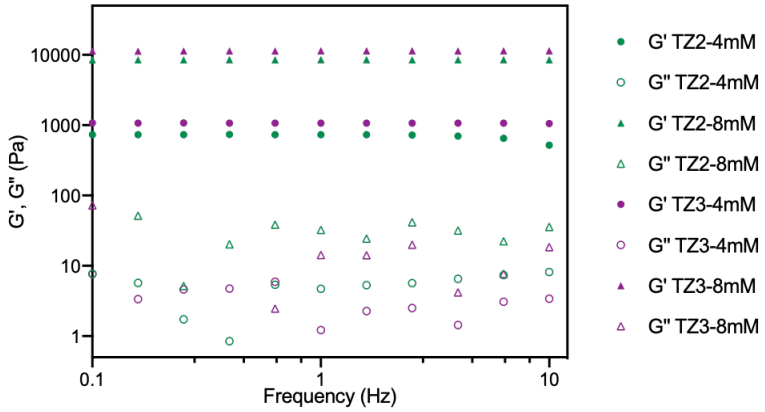

Figure S5.3. Frequency sweep measurements of Tz-Nb-based PEG hydrogels in PBS (pH 7.4) at 37 ± 0.2 °C. Norbornene/tetrazine molar ratios were kept at 1:1 and final PEG macromonomers concentrations were 4 mM and 8 mM, respectively. Frequency sweep data was collected in a range of 0.01 Hz to 10 Hz with strain of 0.05%.

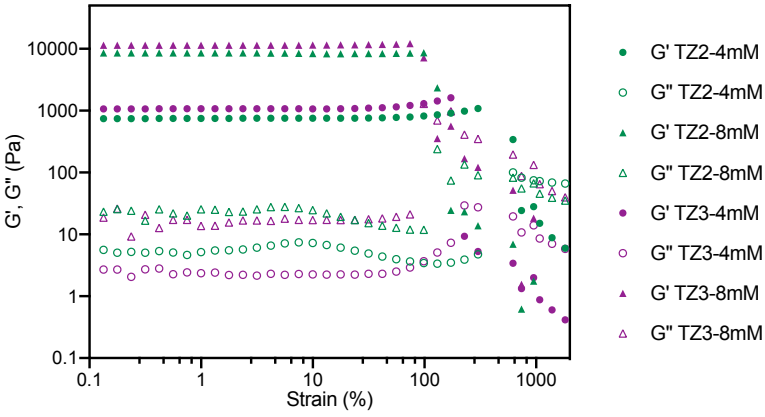

Figure S5.4. Amplitude sweep measurements of Tz-Nb-based PEG hydrogels at 37 ± 0.2˚C with a frequency of 1 Hz and strain from 0.1% to 2000%. Norbornene/tetrazine

molar ratios were kept at 1:1 and final PEG macromonomer concentrations were 4 mM and 8 mM, respectively.

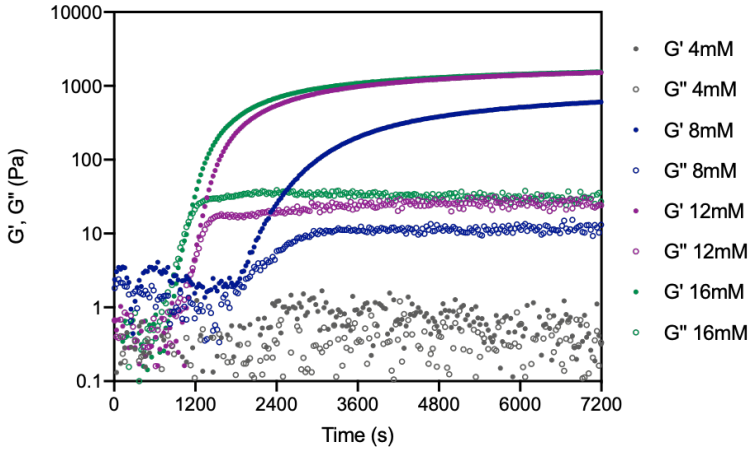

Figure S5.5. Time sweep measurements of Tz1-Nb-based PEG hydrogels at 37 ± 0.2˚C with a fixed frequency of 1 Hz and strain of 0.05%. Norbornene/tetrazine molar ratios were kept at 1:1 and final PEG macromonomer concentrations were 4, 8, 12 and 16 mM, respectively.

5.6.6 Pore size measurement

A fluorescent Tz-Nb-based PEG hydrogel was prepared similarly as described in **5.6.3**. Briefly, a freshly prepared solution of **PEG-NB** (60 µL) was mixed with solution of FITC-RGD (6 µL), vortexed for 10s, and incubated at room temperature for 30 min. Afterwards, a solution of **PEG-TZ1**/**TZ2**/**TZ3** (60 µL) was added and vortexed for 10s to obtain a homogeneous solution with final a PEG macromonomer concentration between 4-10 mM. The precursor solution was then transferred into µ-Slide VI 0.4 (ibidi) and incubated at 37˚C for 2h. Fluorescent images were acquired on Leica SP8 confocal microscope with a resolution of 512 × 512 pixels. An excitation wavelength of 488 nm and an emission filter of 500−545 nm for FITC was applied. The diameters of gas bubbles were measured in Fiji by drawing a straight line horizontally (angle < 3°) with the corresponding scale. Over 100 bubbles were measured for each condition.

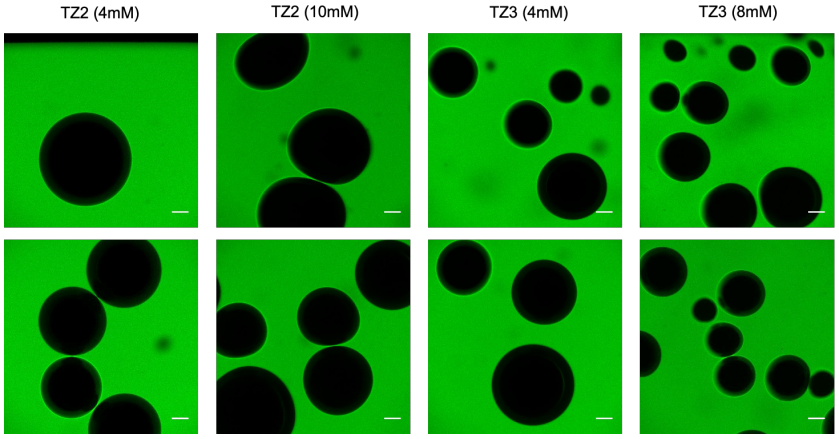

Figure S5.6. Representative images of bubbles formed in Tz-Nb-based PEG hydrogels. Scale bar: 100 µm.

5.6.7 Chondrocytes encapsulation and differentiation

Primary chondrocytes were cultured in DMEM supplemented with bFGF as a monolayer for two passages after isolation from healthy cartilage (Leiden University Medical Center). On the day of 3D cell encapsulation, the chondrocytes were dissociated by incubation with trypsin/EDTA for 5 min. Afterwards, DMEM supplemented with bFGF was added and cells were dissociated with a serological pipet by pipetting up and down. Cells were collected by centrifuge (300 g, 5 min) and resuspended to obtain a final cell concentration of 2 x 10^6 cells/mL. To prepare the hydrogel, a freshly prepared solution of **PEG-TZ1/TZ2 /TZ3** (75 µL) was first mixed with RGD-NB (40 mM, 7.5 µL) by pipetting. After 15 min incubation, a cell suspension (7.5 µL) was added and mixed, followed by the addition of a freshly prepared **PEG-NB** solution (60 µL). The mixture was pipetted into an angiogenesis slide with volume of 12 µL/well. After incubation at 37˚C for 20 min, a fresh DMEM solution containing bFGF (48 µL) was added on top and cells were cultured at 37 °C. After overnight incubation, the encapsulated chondrocytes were treated with freshly prepared chondrogenic differentiation medium (CDM).[6,7]

5.6.8 LIVE/DEAD staining

To evaluate cell viability, LIVE/DEAD staining of the encapsulated cells was performed at pre-determined time points as described in Chapter 4. In brief, cell-laden hydrogels were rinsed twice with PBS (pH 7.4, 45 µL) and incubated with a pre-prepared staining solution (45 µL) (calcein AM (2 µM) and propidium iodide (1.5 µM)) for 30 min to 1 h at 37 °C. After rinsing with PBS twice, the stained cell-laden hydrogel was imaged in a z-stack on Leica TCS SP8 confocal laser scanning microscope equipped with a 10× air objective. Fluorescent images were acquired at a resolution of 1024 × 1024 pixels. An excitation wavelength of 488 nm and an emission filter of 500−545 nm for calcein AM and an excitation wavelength of 532 nm and an emission filter of 594−686 nm for propidium iodide was set. Cell viability was determined by counting the calcein AM-stained green cells (viable) and PI-stained red cells (dead) in ImageJ.

5.6.9 Alcian blue staining

After a 4-day differentiation of the chondrocytes, the cell-laden hydrogels were rinsed with PBS (45 µL x 2) and incubated with 4% paraformaldehyde overnight prior to fixation. After that, the hydrogels were incubated with H_2O for 10 min (45 µL x 3) and afterwards with 3% acetic acid (pH 2.5). The alcian blue staining solution was added on top of the hydrogel and incubated for 3h at 37˚C. The stained hydrogels were washed by incubation with a 3% acetic acid solution for 2h (45 µL x 3) at 37˚C, followed by an overnight incubation with H_2O. Bright field microscopy images were collected on an Olympus microscope with 10x and 20x air objectives.

5.6.10 Appendix: NMR spectra

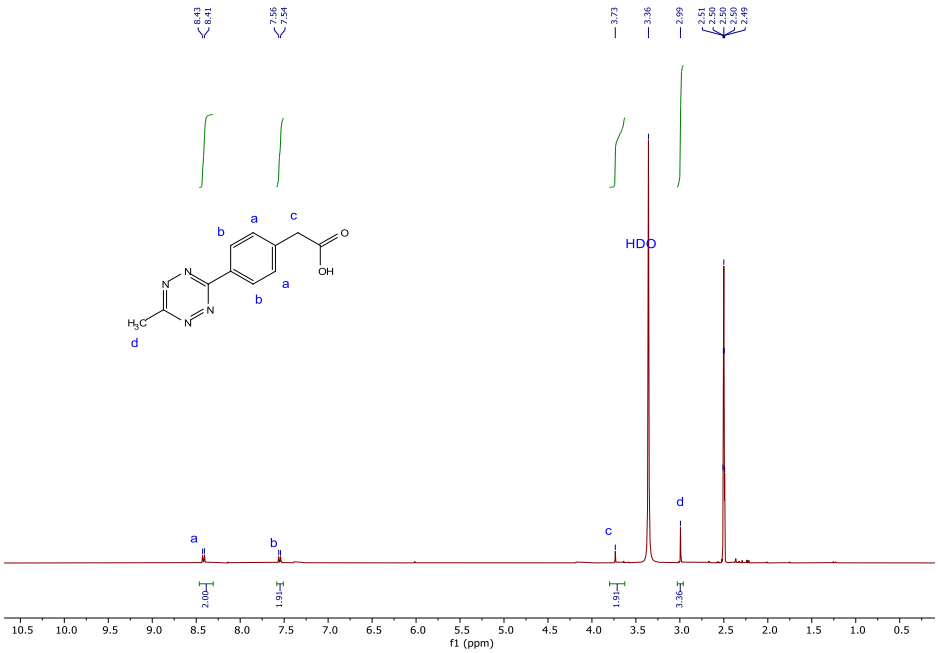

Figure A5.1. ^{1}H-NMR (400 MHz, 298K, DMSO-d_6) spectrum of **TZ1**

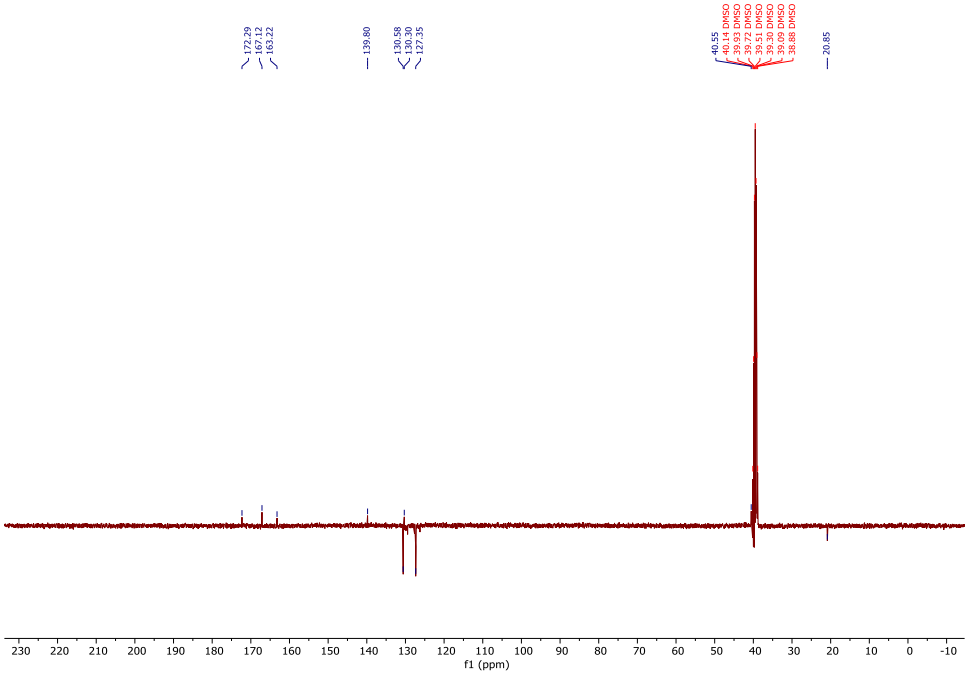

Figure A5.2. ^{13}C-NMR (400 MHz, 298K, DMSO-d_6) spectrum of **TZ1**

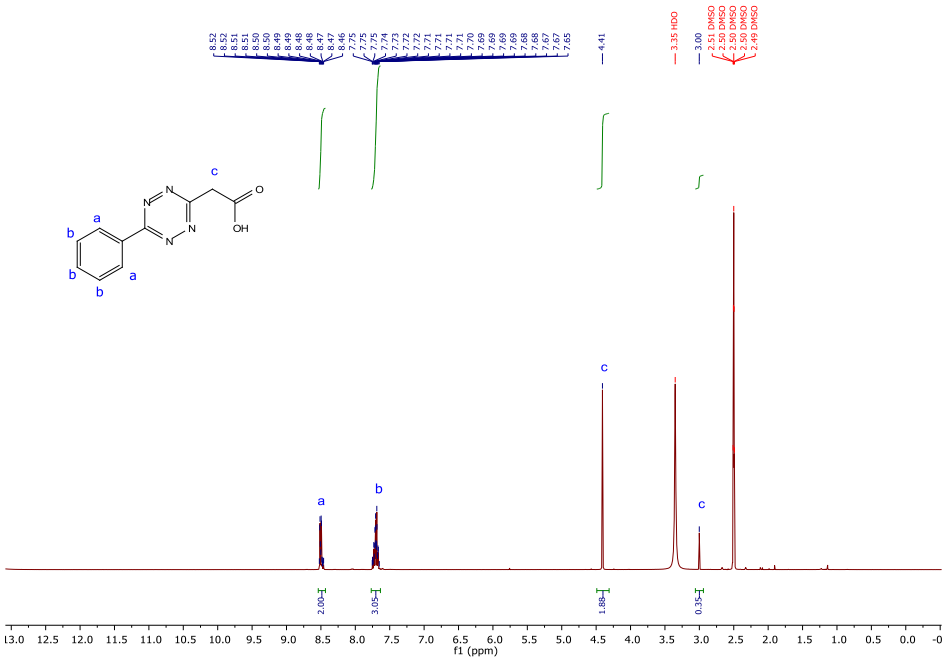

Figure A5.3. ^{1}H-NMR (400 MHz, 298K, DMSO-d_6) spectrum of **TZ2**

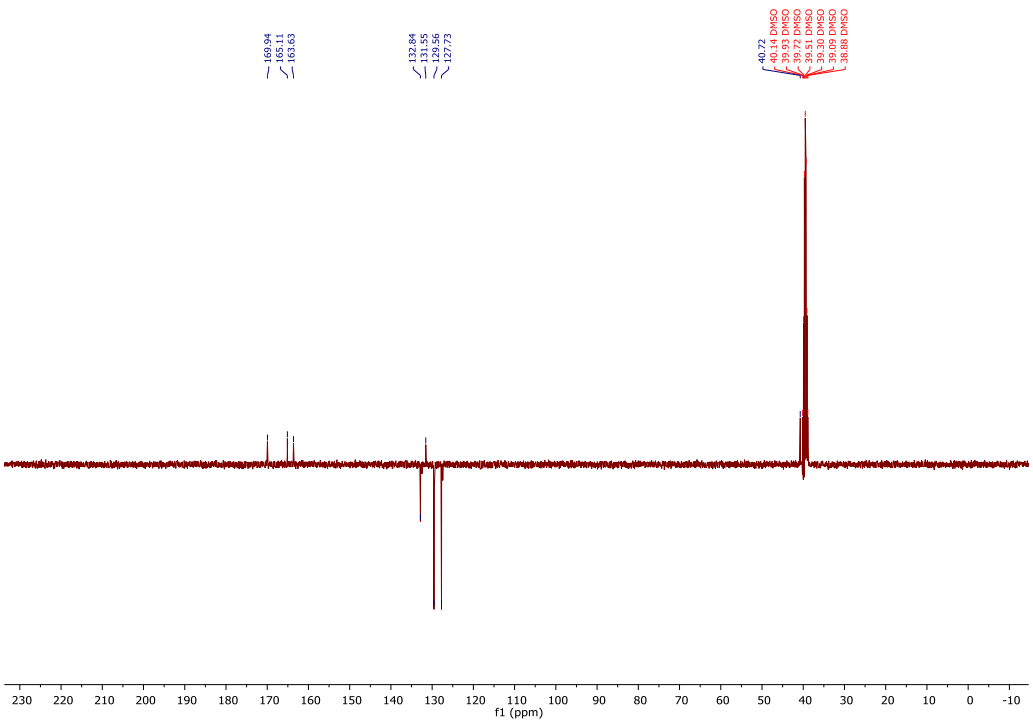

Figure A5.4. ^{13}C-NMR (400 MHz, 298K, DMSO-d_6) spectrum of **TZ2**

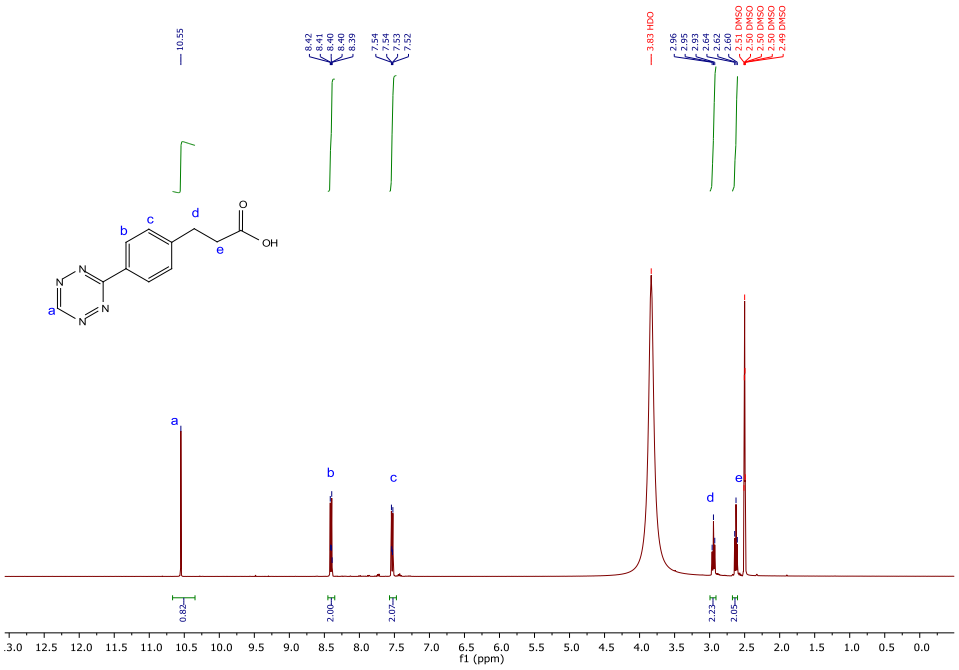

Figure A5.5. ^{1}H-NMR (400 MHz, 298K, DMSO-d_6) spectrum of **TZ3**

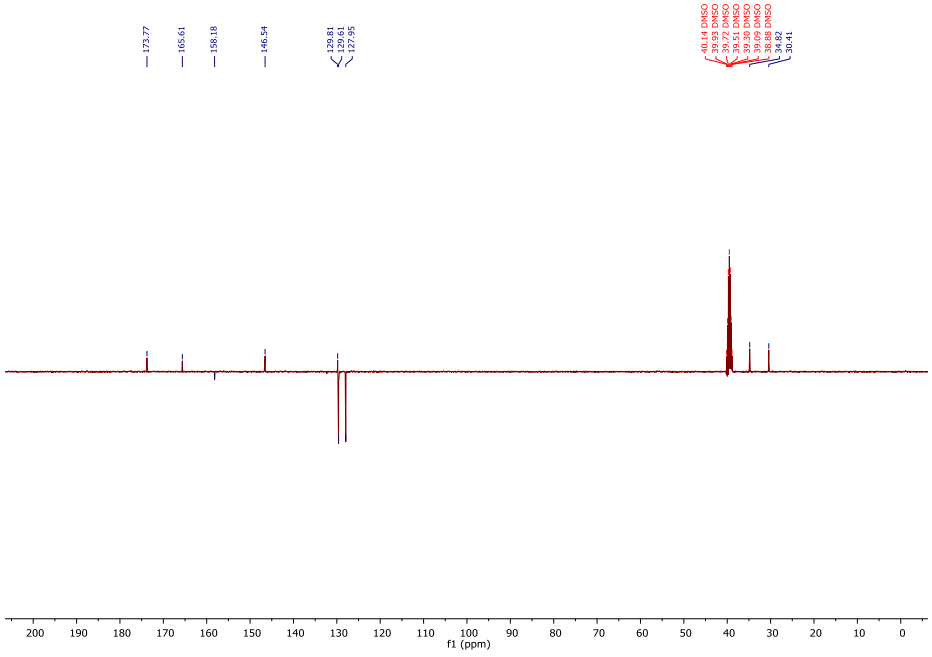

Figure A5.6. ^{13}C-NMR (100 MHz, 298K, DMSO-d_6) spectrum of **TZ3**

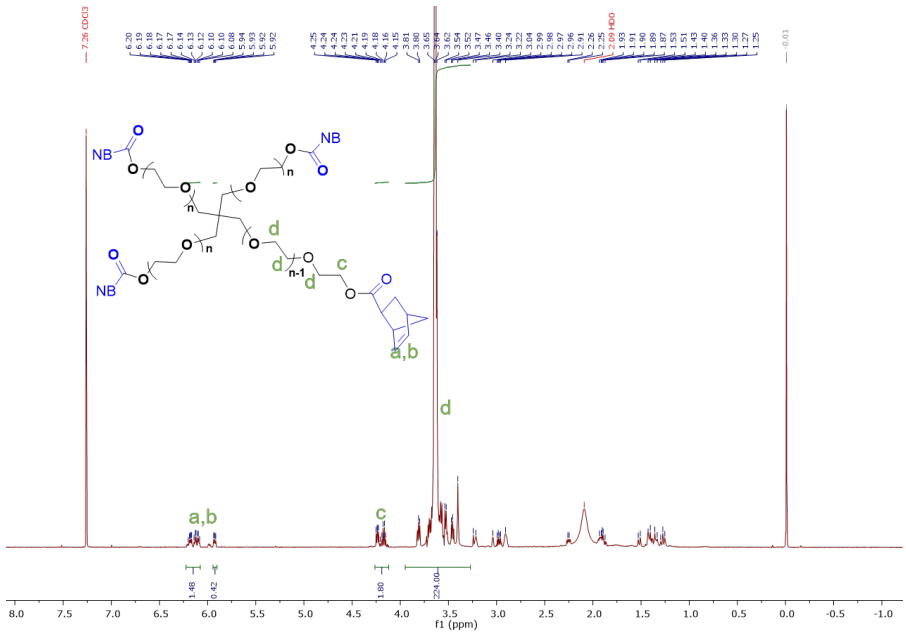

Figure A5.7. ^{1}H-NMR (400 MHz, 298K, $CDCl_3$) spectrum of **PEG-NB**. The degree of functionalization was 90%.

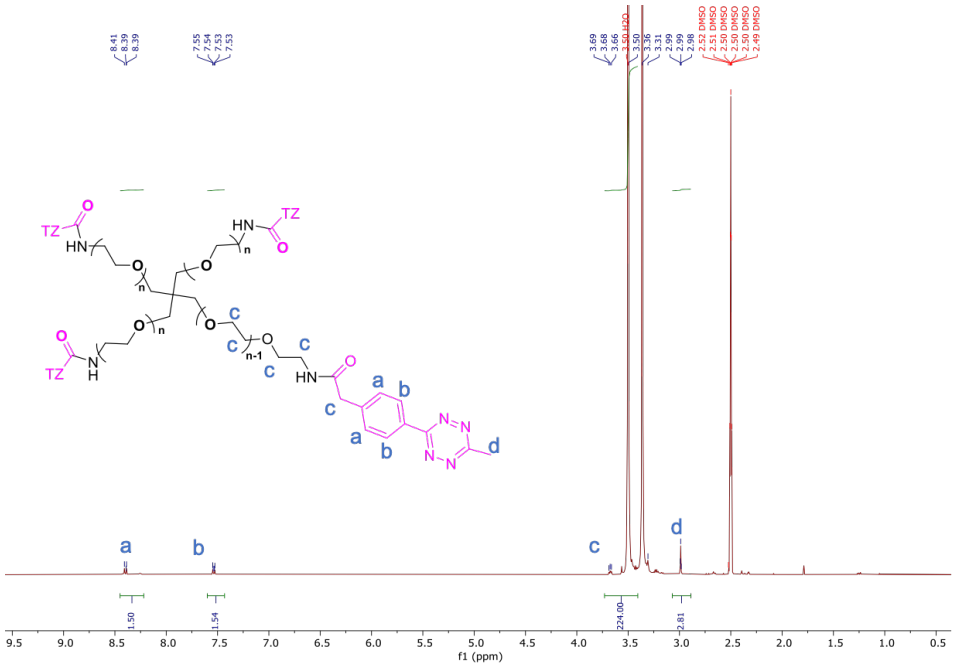

Figure A5.8. ^{1}H-NMR (400 MHz, 298K, $CDCl_3$) spectrum of **PEG-TZ1**. The degree of functionalization was 75%.

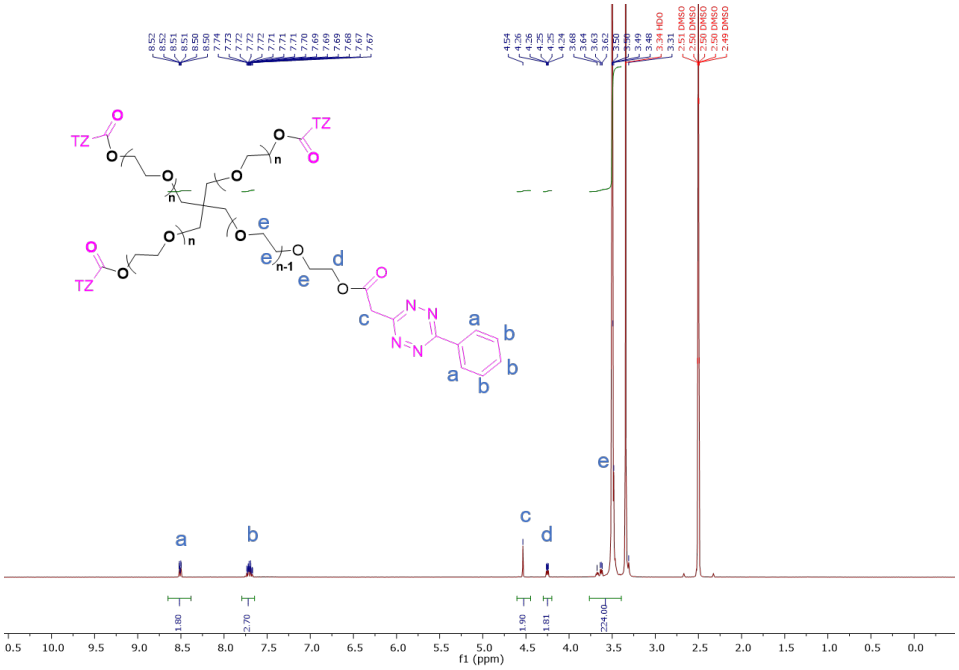

Figure A5.9. ^{1}H-NMR (400 MHz, 298K, DMSO-d6) spectrum of **PEG-TZ2**. The degree of functionalization was 90%.

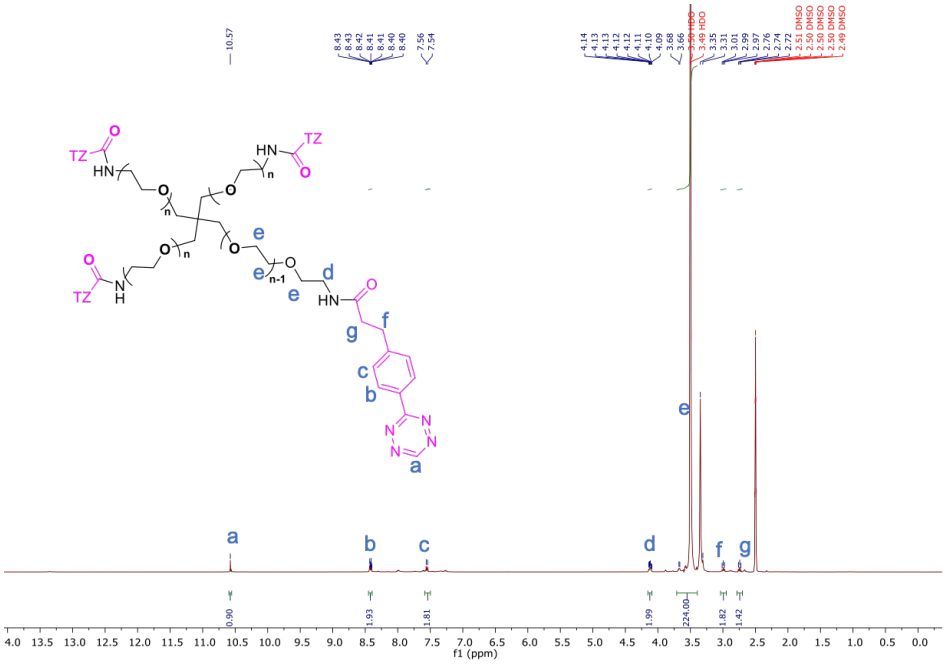

Figure A5.10. ^{1}H-NMR (400 MHz, 298K, DMSO-d6) spectrum of **PEG-TZ3**. The degree of functionalization was 90%.

5.6.11 References

[1] H. Zhan, H. De Jong, D. W. P. M. Löwik, *ACS Appl. Bio Mater.* **2019**, *2*, 2862.

[2] W. Mao, W. Shi, J. Li, D. Su, X. Wang, L. Zhang, L. Pan, X. Wu, H. Wu, *Angew. Chemie - Int. Ed.* **2019**, *58*, 1106.

[3] M. R. Karver, R. Weissleder, S. A. Hilderbrand, *Bioconjug. Chem.* **2011**, *22*, 2263.

[4] N. K. Devaraj, M. R. Karver, S. A. Hilderbrand, R. Weissleder, **2015** *US Patent No. US2015246893A1*.

[5] C. C. Lin, A. Raza, H. Shih, *Biomaterials* **2011**, *32*, 9685.

[6] K. Words, A. Green, **2002**, 338.

[7] C. Carapagnoli, N. M. Fisk, S. Kumar, L. Bellantuono, P. R. Bennett, I. A. G. Roberts, *Blood* **2000**, *96*, 2396.